Vertical wind speed in winter clouds investigated with a triple frequency instrumental setup

R. PIRLOAGA[1], G. CIOCAN[1,2], M. ADAM[1], A. NEMUC[1,*]
[1]*National Institute of Research and Development for Optoelectronics INOE 2000, Magurele, 077125, Romania*
[2]*Faculty of Physics, University of Bucharest, Magurele, 077125, Romania*

The paper presents the first investigation of the clouds' dynamics over the 2024-2025 winter season in Magurele, Romania. The vertical wind speed provided by a Doppler wind lidar (DWL) and two Doppler cloud radars (DCR) is analysed. Four case studies are shown which refer to two low- to mid-altitude clouds (both ice and mixed phase cloud), a high-altitude cloud (mostly ice cloud) and one extended towering cloud (mostly ice cloud). While the same analysis was performed on all cases, only the 11 December 2024 example is detailed in the main text whereas the remaining cases are provided in annexes. In the selected case studied, the vertical speed determined from DWL is slightly higher than the speed determined from the two DCR, especially in the mixed phase region (upper part of the cloud) which shows the DWL capability to better sense this type of cloud. The correlation coefficient between the wind speed determined by DWL and a DCR is 0.78 (RPG) and 0.75 (MIRA) for the low- to mid-altitude cloud on 11 December 2024. For the high-altitude cloud, the correlation between DWL speed and DCR speed is 0.54 (both radars) could be due to the fact that DWL is not capable of sensing the entire cloud. DWL can provide valuable information of finer structures in a mixed phase region of a low to mid-altitude cloud, the final vertical speed profile should be considered based on information received from both the DWL and a DCR. This study highlights the value of combining Doppler wind lidar and Doppler cloud radar measurements to improve the characterization of vertical cloud dynamics across various types of clouds and altitude ranges during winter conditions.

(Received July 13, 2025; accepted February 4, 2026)

Keywords: Vertical wind speed, Winter clouds, Doppler wind lidar, Doppler cloud radar

1. Introduction

Investigating cloud dynamics is vital for advancing atmospheric modelling, as it directly impacts the accuracy of weather forecasts, the reliability of climate simulations, and the understanding of cloud-related processes such as precipitation formation and energy transfer within the atmosphere [1].

Vertical speeds in clouds are a key-element that generates uncertainties in the climate system while their role in climate and numerical prediction models have been often understated [2]. Vertical speeds are an important factor that facilitates development, evolution and transformation of clouds and therefore, a good estimation of the vertical cloud dynamics is needed. High quality resolution data of vertical speeds are detected using ground-based optoelectronics instruments such as Doppler Wind Lidar (DWL). This instrument is capable of detecting vertical speeds, provided that atmospheric scatterers are present. The scatterers can be any particle that interacts with laser radiation emitted by the lidar (e.g. aerosols, insects and most important: cloud particles). The instrument presents some limitations such as in the presence of rain or large ice particles when laser radiation is attenuated and echo signals are contaminated. For optimal results, a synergistic approach involving one Doppler Wind Lidar (DWL) and two Doppler Cloud Radars (DCRs) is employed to enable a comprehensive analysis of cloud vertical speeds, independent of cloud microphysical properties that may otherwise distort the measurements.

Doppler Radars were used in the past to detect cloud related vertical speeds and to validate models [3], to observe updrafts, downdrafts and turbulences [4] or to detect vertical air motions in stratiform clouds [5]. Lately, studies have started using DWL to evaluate vertical winds near and inside a cloud deck [6] or to detect updraft and downdraft in cumuli clouds [7].

Buhl et al. (2015) [8] have studied the vertical speed in Planetary Boundary Layer (PBL) and clouds using a DWL, a DCR and a wind profiler. The authors showed that turbulent air motion or the vertical movement of falling ice and water particles can be measured at once while a coherent picture of different kinds of vertical motions in the atmosphere can be drawn. By means of the wind profiler (which determines the air speed), the unbiased fall speed of particles (terminal speed) can be measured. Buhl et al. (2015) [8] underscore the critical role of the Doppler Wind Lidar (DWL), highlighting its capability to detect cloud and aerosol particles that remain undetectable by conventional cloud radar or wind profiler systems.

Peng et al. (2024) [9] studied the marine wind by DWL and DCR. The study focuses on the maximum detection range of lidar and microwave radars at different bands. While DWL can detect winds based on backscatter radiation from small particles, DCR can detect high winds based on backscatter radiation from large particles. In the

presence of high particle concentrations, lidar signals are attenuated due to scattering and absorption effects, resulting in weakened return signals. The authors conclude that lidar and radar systems provide complementary capabilities across a range of wind speeds under clear-air conditions.

The detection range for a DWL is smaller in precipitation while high frequency (W-band) radars can perform better on foggy days and low frequency radars (Ka-band) on rainy days. From the perspective of all-weather conditions, the authors recommend the W-band radar to be combined with lidar.

Barbaresco et al. (2015) [10] studied the mean wind field, turbulences, and aircraft woke vortices using Doppler wind lidar, X-band Doppler radar and UV direct detection lidar. Their study was developed for improving air traffic safety and operations. Their results demonstrate strong agreement between vertical radar and lidar measurements, confirming the feasibility of these instruments for generating Eddy Dissipation Rate maps and for detecting the influence of wake vortices on raindrop behaviour.

In this study, we investigate the capability of a DWL and two DCR (high frequency W-band and low-frequency Ka-band) to sense various clouds and determine the vertical speed in cloud. The cloud particles detection depends on the emitted wavelength from the instrument and thus, we want to explore their efficiency in different types of clouds. Recent investigation over the wind field in Magurele, Romania (at MARS-Magurele center for Atmosphere and Radiation Studies) tackled the PBL turbulence using the DWL [11] where the wind field is determined based on aerosol backscattering**.**

The rest of the paper is organised as follows. The Instruments section describes the RADO-Bucharest Cloudnet site and outlines the specifications and deployment of the Doppler-Wind-Lidar together with the two Doppler Cloud Radars. The Methodology section details the processing workflow, covering the selection of winter case studies, application of Cloudnet target classification, creation of cloud masks, and the spatial-temporal alignment of the three data sets. The Results section presents the measurements, comparing the vertical-speed profiles obtained by each instrument in mixed-phase and ice-phase clouds, and quantifies their consistency through speed-difference plots and regression analysis. It also interprets the patterns observed, noting each instrument's strengths, the identified biases, and how lidar penetration depth is limited by cloud optical thickness. The Conclusions section condenses the key findings and explains how combining lidar and radar data can refine future retrievals and supply reliable reference data for forthcoming satellite missions.

2. Instruments

In this study we employ a HALO Photonics DWL and two DCR (RPG-FMCW-94 and DCR MIRA35s) which are described below. All instruments are currently deployed at RADO-Bucharest Cloudnet Station (https://cloudnet.fmi.fi/) [12] part of ACTRIS Centre for Cloud Remote Sensing (https://www.actris.eu/topical-centre/ccres). RPG cloud radar is the property of ESA and is also part of FRM4RADAR (https://geomet.uni-koeln.de/forschung/frm4radar). The location is 6 km South of Bucharest, Romania, in a peri-urban area. The instruments are operated under strict regulation, maintenance and calibration procedures in order to obtain best quality cloud data being in the process of labelling for ACTRIS/CCRES (https://actris-nf-labelling.out.ocp.fmi.fi/facility/99). Continuous, high-resolution data are provided by all three instruments since December 2019 with small gaps during maintenance, calibration procedures, power outages or field campaign deployments. The location of the three instruments is shown in Fig. 1, which is also part of MARS (44.3° N, 26.1° E, 70 meters ASL). Meteorologically, the area is characterised by warm summers and humid continental climate where seasonal variation in precipitation is minimal (Köppen–Geiger climate classification type Dfa) and for more information, please refer to [11,12]. The site has also other relevant instrumentation for atmospheric research [13-16].

DWL is a Streamline XR model manufactured by Halo Photonics/Lumibird and further developed and distributed by Metek GmbH-Fig. 1(a). The wind lidar system operates at an eye-safe wavelength of 1.5 μm on vertical and scanning scenarios. In order to produce high quality information about vertical motions of the atmospheric particles, the instrument is operated continuously at 30 meters vertical spatial resolution and approximately 6 seconds time resolution, up to a maximum altitude of 12 km above ground. The main retrievals from DWL are the attenuated backscatter coefficient and radial speed. Further postprocessing of these parameters, along with a scanning scenario allows the calculation of wind components, PBL characteristics or turbulent mixing sources [11]. In this study, only the vertical retrievals are involved to analyse several case studies. Consequently, in this study, the radial speed is interchangeable with vertical speed.

One of the two DCR used for this analysis is a RPG-FMCW-94 model manufactured by RPG Radiometer physics GmbH-Fig. 1(b) (RPG). This frequency-modulated continuous wave radar operates at 94 GHz frequency (approximately 3.19 mm wavelength - W band) at approximately 3 seconds time resolution and a variable spatial resolution ranging from 27.1 meters close to ground level up to 51.1 meters at high altitudes (from ~ 10 to ~ 15 km).

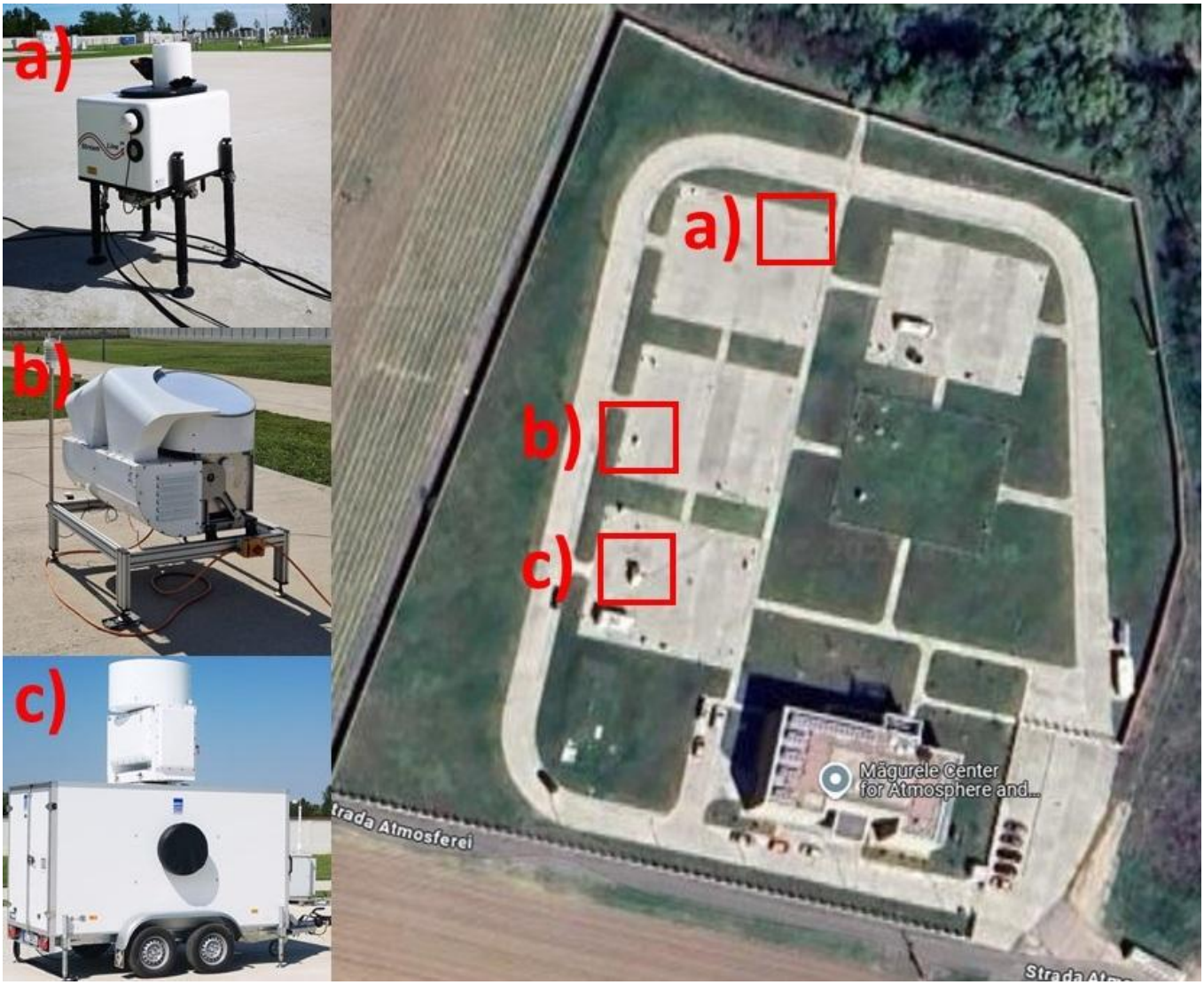

Fig. 1. Illustration-aerial view of MARS (right photo) showing the ground-based cloud remote sensing infrastructure with a) Doppler wind lidar, b) RPG cloud radar and c) MIRA cloud radar (left close up photos of the instruments). Image based on Google Maps (https://www.google.com/maps) (colour online)

The other DCR is a MIRA35s model manufactured by Metek GmbH-Fig. 1c (MIRA)). This radar operates at 35 GHz frequency (approximately 8.56 mm wavelength - Ka band) under pulsatory regime. This DCR is operated at a 5 seconds time resolution and an approximately 31 meters spatial one. Similar to the DWL, a scanning system is mounted on the radar but in this study, we only use the vertical measurements scenario.

The main retrievals from DCRs are radar reflectivity and radial speed. With further processing of DCR data one can estimate Doppler spectra, skewness or linear depolarization ratio in order to obtain enhanced information regarding turbulences in the atmosphere, shape of particles or cloud microphysics [17-19]. Data for the current study is available on [20].

2. Methodology

This article is focusing on several case studies in order to analyse the dynamics in low to mid-altitude and high-altitude clouds. In the first step, we use CLOUNET Target classification algorithm developed by [21] to select a cloud. Next, we start estimating the dynamical behaviour (vertical wind field) of the cloud using the three doppler instruments described in Section 2. The target classification consists of 10 categories: (1) cloud droplets, (2) drizzle or rain, (3) drizzle/rain and cloud droplets, (4) ice, (5) ice and supercooled droplets, (6) melting ice, (7) melting ice and cloud droplets, (8) aerosols, (9) insects, or (10) aerosols and insects. For this study only the first 7 categories are considered (Fig. 2 - top). Furthermore, we grouped all the 7 classes into 3 conventional categories: ice (class 4), liquid (classes 1, 2 and 3) and mixed-phased (5, 6 and 7). The white regions represent the absence of particles in the atmosphere or the presence of particles classified as 8, 9 and 10 categories which were not considered (Fig. 2 - bottom). The selection of the minimum altitude, maximum altitude, start time and end time of the cloud was performed case by case by visual inspection analysing five months of cloud data (November

2024—March 2025). A total number of four case studies was selected from the investigated period, with two cases of clouds under 4200 meters altitude, one case of a 6000-8000 meters altitude cloud and 1 case of a cloud with large vertical extent (2500-8000 meters altitude). In these cases, cloud temporal extent varies from 3 to 6 hours.

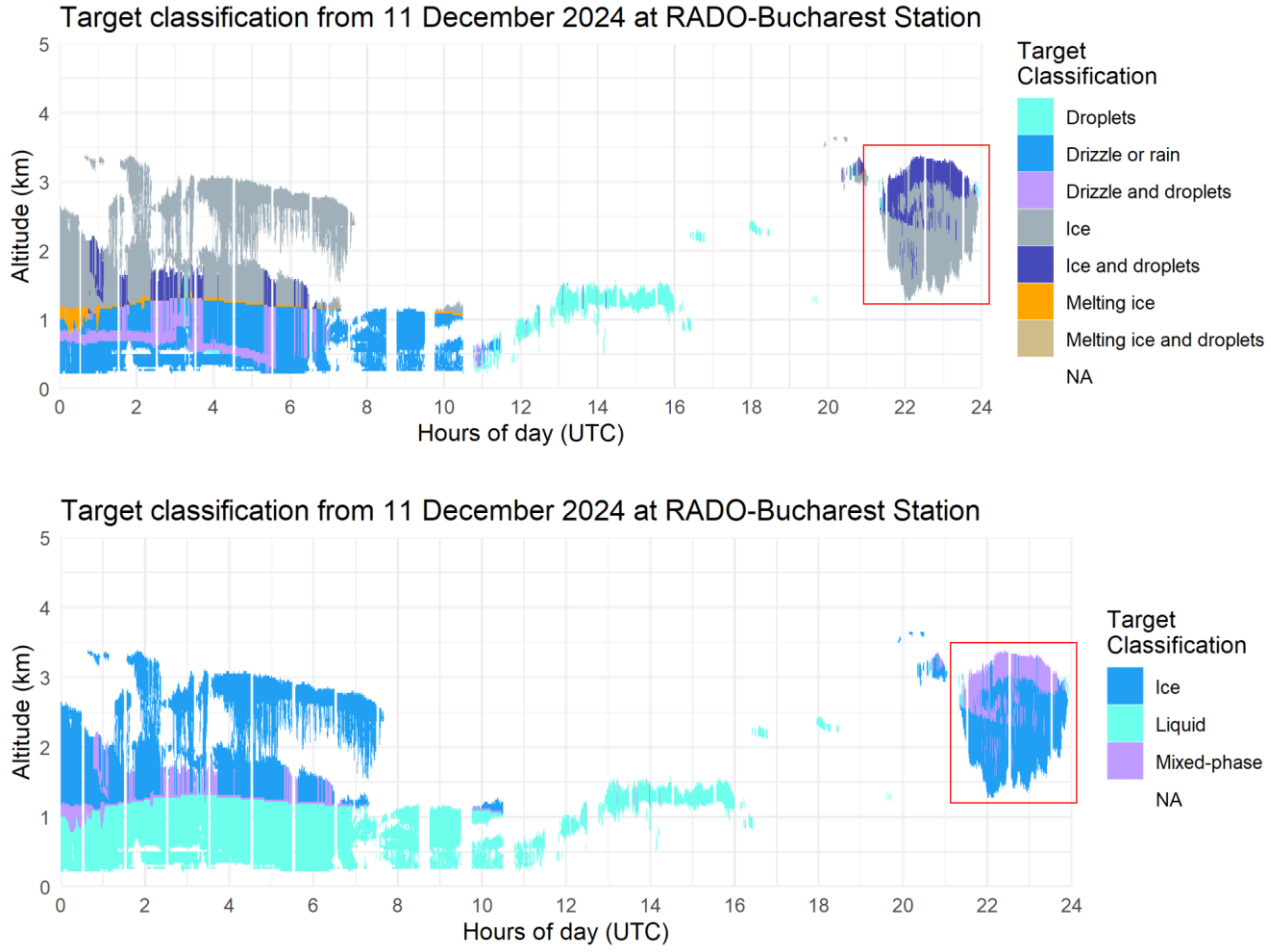

Fig. 2. Target classification of clouds (aerosol classes are not considered) for 11 December 2024 at RADO-Bucharest station (colour online)

To enable a consistent comparison across all instruments, the vertical speed profiles from the DWL and the two DCRs (Fig. 3) were resampled to a common spatial and temporal resolution of 30 meters and 30 seconds, as shown in Fig. 4. This was achieved by averaging multiple consecutive profiles from each instrument, depending on their native time resolution: approximately 6 seconds for the DWL, 3 seconds for the RPG DCR, and 5 seconds for the MIRA DCR. White stripes (NaN values) appear at certain time intervals due to the cloud mask which in turn depends on DWL input data (with gaps due to scanning periods).

For spatial consistency, we standardised the vertical resolution to 30 meters across all data sets. While the DWL already operates at this resolution, the DCR data - originally recorded at variable vertical resolutions - were interpolated vertically using a standard interpolation function to match the DWL's grid. This approach ensures all data are aligned on a unified vertical and temporal grid, allowing for a direct comparison of vertical speed profiles across instruments.

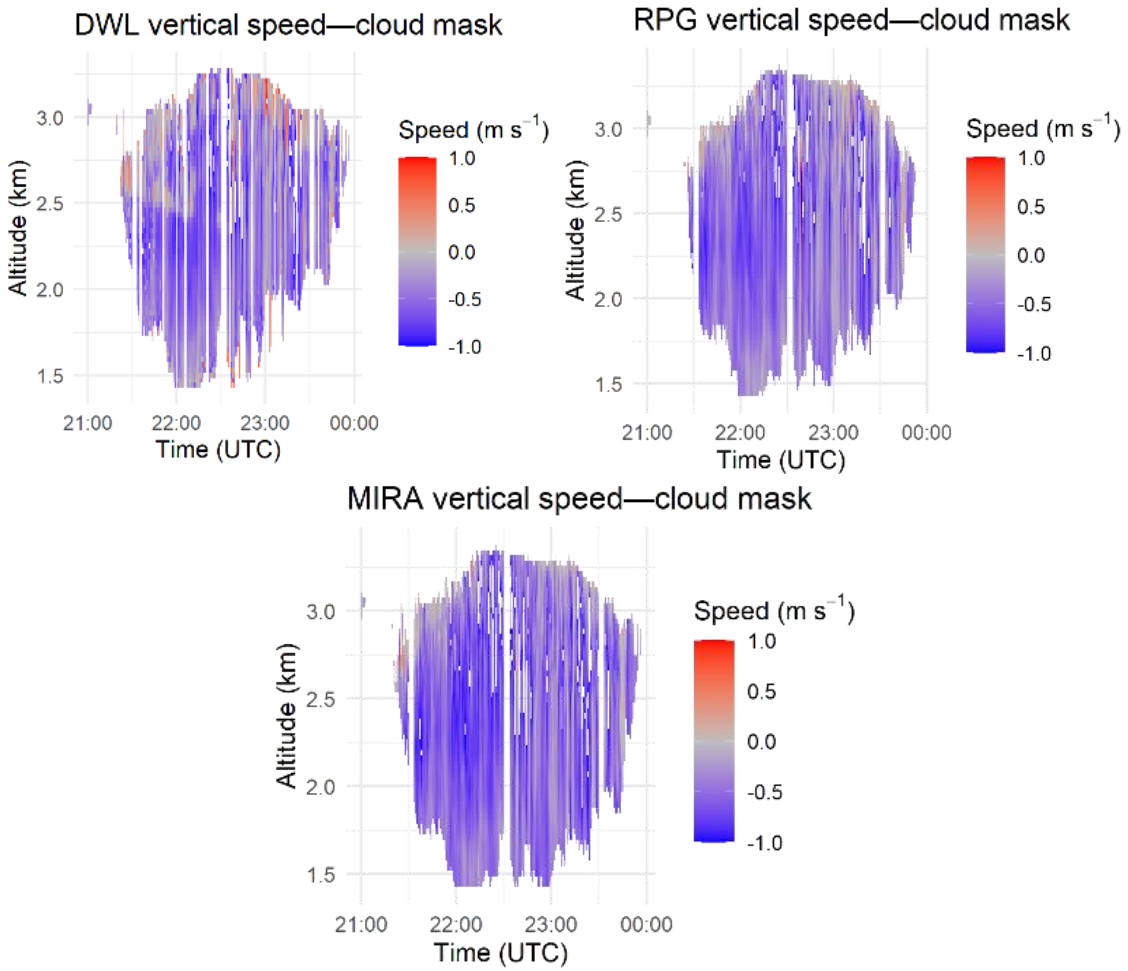

Fig. 3. Cloud masked vertical wind speed measured by DWL (top), RPG cloud radar (middle) and MIRA cloud radar (bottom) for low to mid-altitude clouds (1400—3500 meters altitude) in the 21:00—24:00 time interval on 11 December 2024 (colour online)

A "cloud mask" was created using the Target classification data containing ice, liquid or mixed categories. The mask was applied to DWL, MIRA and RPG wind data to eliminate any other particles that could contaminate the data (aerosols or insects). Furthermore, cloud mask was divided into "ice" and "mixed" particles to separate and analyse the cloud with respect to its phase (liquid class was not present in any of the selected cases).

The DWL data, especially in the mixed phased part of the cloud, measured some vertical speed values outside the range (we speculate that the values are due to multiple scattering). These data were eliminated, by removing values outside the 0.05th–99.95th percentile range. Pearson correlation coefficient of vertical speed was calculated for all three combinations of Doppler instruments (DWL-RPG, DWL-MIRA and MIRA-RPG) while a linear regression model was used to estimate the linear fit between them (to check for inconsistency and to quantify the differences among instruments). Vertical speed differences between instruments for every grid point are shown in Fig. 5 for the same temporal and spatial intervals as for Fig. 4.

3. Results

Fig. 2 shows a cloud measured between 21:00—24:00 UTC on 11 December 2024 in the 1400—3500 meters altitude region above ground. The cloud displays a specific structure of mixed phased particles predominantly on upper part of the cloud (above 2500 meters) and ice particles on lower part of the cloud (below 2500 meters), the two types of particles coexisting between 2500- and 3000-meters altitude (more visible in the first half of analysed period, 21:00-22:30 UTC). A similar pattern is shown in Fig. 3 which represents a magnified portion of the cloud structure. Positive values in the mixed phase part of the cloud and negative values on ice part are more visible on DWL vertical speed time series. The pattern of the updraft structure can also be partly seen in the DCR data, although with smaller values compared to DWL.

A maximum of 1.4 m/s is measured by DWL for the upward speed data at 2790 meters altitude at 21:25:30 UTC and a minimum of -1.9 m/s is measured by MIRA DCR for the downward speed data at 2910 meters altitude at 23:24:00 UTC.

The negative speed (downdrafts) in the ice region (lower part of the cloud) is a characteristic for gravitationally falling of the heavier ice particles. On the

other hand, in the mixed phase (upper part of the cloud), the supercooled liquid droplets are specific for updrafts (positive speeds) which carry moist air and allow droplets to form and further to develop in ice nucleation [22].

The capability of the DWL to catch the updrafts can be better revealed in the speed difference between DWL and DCR (Fig. 5). Buhl et al. (2015) [8] also mentioned that the DWL can deliver critical information about the vertical speed of small cloud droplets and their fast-changing turbulent motion.

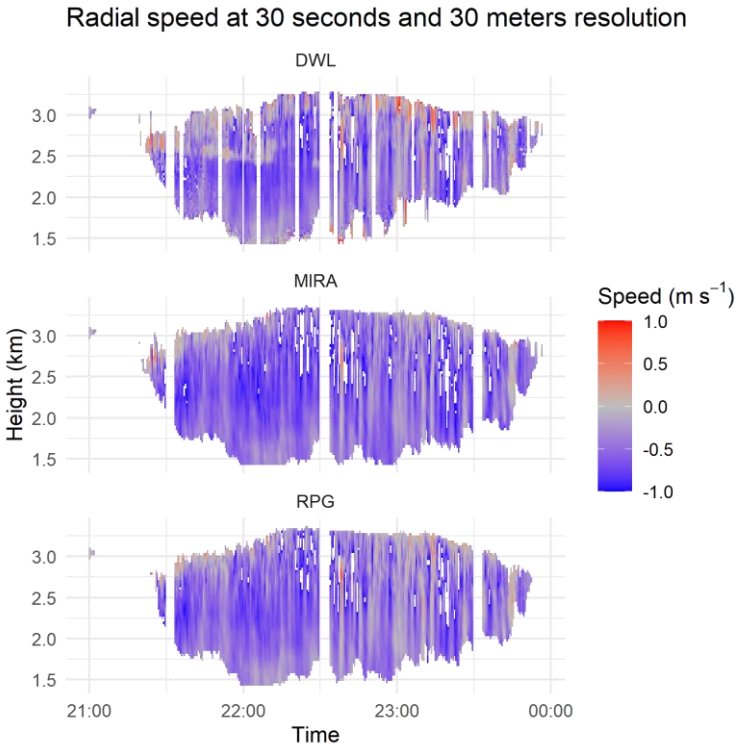

Fig. 4. Vertical speed profiles interpolated at the common resolution (30 seconds and 30 meters) for low to mid-altitude clouds (1400—3500 meters altitude) in the 21:00—24:00 time interval on 11 December 2024 (colour online)

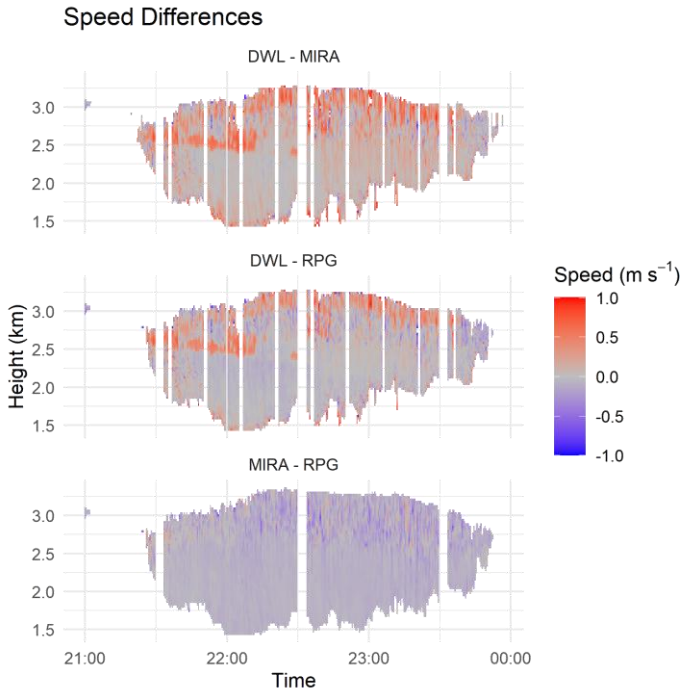

Fig. 5. Speed differences between DWL and MIRA radar (top), DWL and RPG radar (middle), MIRA and RPG radars (bottom) for low to mid-altitude clouds (1400—3500 meters altitude) in the 21:00—24:00 time interval on 11 December 2024 (colour online)

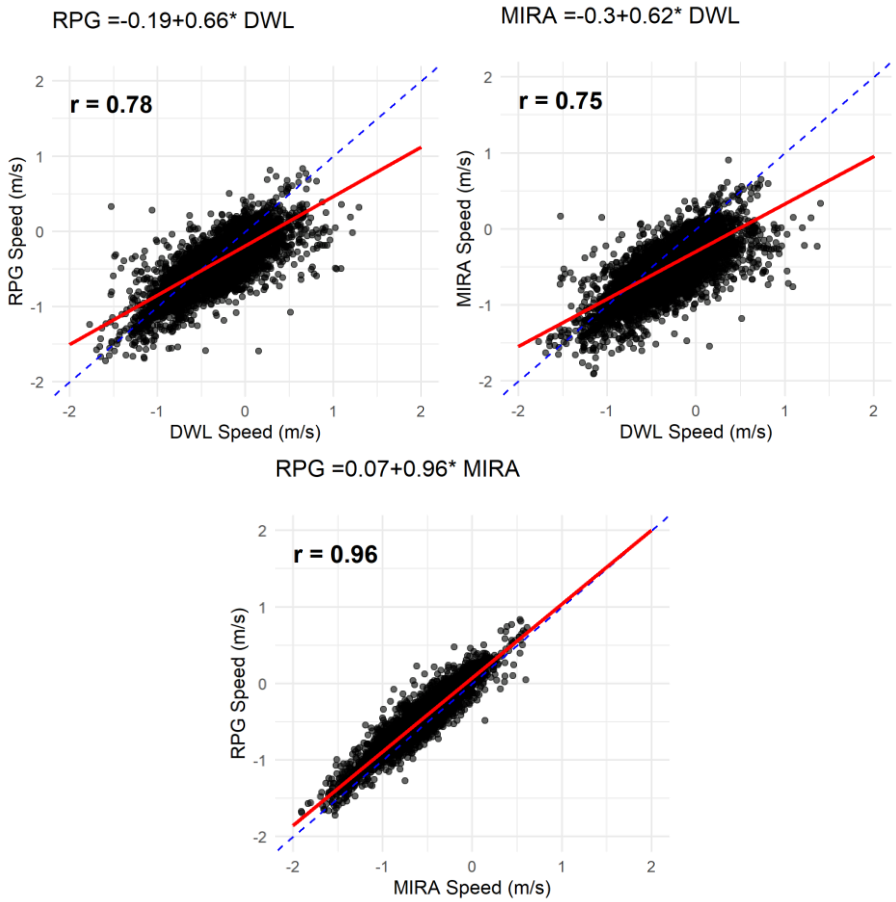

Fig. 6. Correlation graph between DWL and RPG radar (top), DWL and MIRA radar (middle), MIRA and RPG radars (bottom) for low to mid-altitude clouds (1400—3500 meters altitude) in the 21:00—24:00 time interval on 11 December 2024 (colour online)

The differences between MIRA and RPG are significantly smaller (Fig. 5 bottom). The overall analysis clearly shows that DWL measures vertical speed of mixed phase particles more efficiently (top part of the cloud where differences between DWL and DCRs are greater than 1 m/s), while the synergy of DWL and DCR is more efficient for falling particles (middle to low part of the cloud) where differences between DWL and DCRs are very small (close to 0 m/s), result which was quantified as well by Buhl et al., 2015 [8].

In order to quantify the differences among instruments for determining the vertical speeds, we performed a regression analysis. The scatter plots are shown in Fig. 6. The correlation coefficients for the analysed cases are shown in Table 1, along with the time and space delimitations of the clouds.

In average, there is a distinct overestimation of DWL vertical speeds in all case studies compared with DCRs. We have overall good correlations between DWL and RPG cloud radar (maximum of 0.78 for 11 December 2024 and minimum of 0.54 during 14 February 2025). A similar good correlation is present in the DWL and MIRA analysis (maximum of 0.74 on 11 December 2024, and a minimum of 0.54 in 14 February 2025 - same days as DWL-RPG correlations). There is a very strong correlation between DCRs (over 0.88 for all case studies).

There exists a specific correlation pattern in the DWL-DCR data on one hand and DCR-DCR data on other hand, in some days where the correlation between radars is the strongest, the correlation with DWL is weakest related to the rest of the correlation values. Vice versa, when the DWL-DCRs is strongest, the correlation between DCRs is slightly smaller. Based on information about ice effective radius and droplet effective radius we observed that the correlation coefficient between DWL and DCR is higher when the droplet particles are present. See for example Fig. A1 for the case of 11 December 2024. We observe high ice size (up to ~ 50 μm) and relatively high droplet size (up to ~ 20 μm). For 12 December 2024 case, we have smaller ice size (less then ~45 μm) and smaller droplet size (~5 μm). For the last two cases, the clouds are mostly ice with ice effective radius of ~ 30-40 μm (18 December 2024) and up to ~ 50 μm (14 February 2025). Ice and droplet radius plots are shown only for 11 December 2024 (Fig. A1).

We noticed a systematic bias for the vertical speed between RPG and MIRA, present on all analysed cases. Thus, the RPG winds are slightly larger by ~ 0.07-0.08 m/s (see the slope in the regression line). In turn, the correlation between DWL and RPG is slightly better than the one between DWL and MIRA (e.g., Fig. 6 and Fig. A2).

The low correlation for the last cloud investigated (14 February 2025) may be due to its big spatial extent, reaching altitudes around 8000 m. Thus, we observed that DWL did not penetrate all the way up on top of the cloud (the laser beam being attenuated). We observed that the ice effective radius was larger in the lower part of the cloud which contributed to a higher attenuation of the laser.

We performed also a regression analysis for the two different cloud components (ice and mixed phase) in order to investigate if there is a better correlation for a specific component (see Annex A). The results for 11 December 2024 are shown in Fig. A2 while the speed differences are shown in Fig. A3-A5. For a better comparison we added again the case for all the particles (already discussed). In this particular case, we observed a better correlation for the ice case. However, for 12 December 2024, the correlation was slightly better for the mixed phase (smaller droplet size). Overall, the slope is closer to unity for 11 December case (for all components).

Table 1. Correlation coefficients for vertical speed between different instruments, along with the temporal and spatial delimitation of the clouds

Date	Cloud duration (UTC)	Height (km)	DWL-RPG	DWL-MIRA	MIRA-RPG
11.12.2024	21:00-24:00	1.4 - 3.5	0.78	0.75	0.96
12.12.2024	00:00-06:00	1.5 - 3.5	0.67	0.67	0.89
18.12.2024	15:00-18:00	6 - 8	0.62	0.57	0.98
14.02.2025	13:00-18:00	2.5 - 8	0.54	0.54	0.99

The other cases are shown in Annex B considering all the particles (no separation between ice and mixed phase). Thus, we show the vertical speed based on cloud mask (Figs. B1, B5 and B9), the vertical speed at the common resolution (Figs. B2, B6 and B10), the speed differences (Figs. B3, B7 and B11) and the correlation graphs (Figs. B4, B8 and B12). As seen in Table 1, the correlation coefficient is lower for 12, 18 December 2024 and 14 February 2025 and this is directly related to weaker contribution of the droplets in the clouds. Also, the slope deviates more from unity.

4. Conclusions

The current study presents the first investigation on the vertical speed profiles in a few types of clouds during the winter of 2024-2025 using three ground-based remote sensing instruments: a DWL, and two high-frequency DCR. Based on these case studies, the following remarks are made:

- The DWL is able to outline finer structures in a mixed phase region of a low to mid-altitude cloud. Thus, for this type of cloud, the final vertical speed profile should be considered based on information received from both the DWL and a DCR.
- In a thick cloud, the laser radiation is partly attenuated and thus DWL cannot sense the entire cloud. Consequently, a DCR is recommended for wind speed evaluation.
- The correlation coefficients between DWL and the two DCR are good in general but significantly lower (around 0.5) in the case of thick clouds.
- We observed a systematic bias between the RPG and MIRA vertical speeds (~ 0.08 m/s) with RPG speed larger while RPG speed correlates better with DWL. Thus, in line with [9] we recommend a synergy between DWL and RPG for a better characterisation of the vertical wind field.

This study provides constructive insights for validating future EarthCARE satellite radar Doppler speed measurements [23] and refining the radar EarthCARE synthetic data in CloudNET, by delivering synergistic ground-based vertical speed reference profiles (DWL + DCR) and characterizing instrument performance and limitations under specific cloud conditions.

Further investigation envisages the study of the clouds over a full year and see under which conditions one instrument performs better than another. A combined vertical speed profiles based on data provided from DWL and one DCR is part of the near future study.

A complete, enhanced understanding of vertical cloud dynamics could be further used for improving atmospheric and climate models and to validate satellite data.

Data availability

The data used in this study are generated by the Aerosol, Clouds and Trace Gases Research Infrastructure (ACTRIS) and are available from the ACTRIS Data Centre using the following link: https://doi.org/10.60656/d4ac16dafcb447b2.

Acknowledgements

This work was carried out through the Core Program within the National Research Development and Innovation Plan 2022-2027, with the support of MCID, project no. PN 23 05/ 3.01.2023. We acknowledge ACTRIS and Finnish Meteorological Institute for providing the data set which is available for download from https://cloudnet.fmi.fi. Measurements were supported by the European Space Agency through the FRM4RADAR project (ESA Contract No. 4000122916/17/I-EF). We acknowledge ECMWF for providing IFS model data.

References

[1] R. A. Houze, International Geophysics **53**, San Diego, Academic Press, 2010.
[2] L. J. Donner, T. A. O'Brien, D. Rieger, B. Vogel, W. F. Cooke, Atmos. Chem. Phys. **16**(20), 12983 (2016).
[3] J. Tonttila, E. J. O'Connor, S. Niemelä, P. Räisänen, H. Järvinen, Atmos. Chem. Phys. **11**(17), 9207 (2011).
[4] P. Kollias, B. A. Albrecht, R. Lhermitte, A. Savtchenko, J. Atmos. Sci. **58**(13), 1750 (2001).
[5] M. D. Shupe, P. Kollias, M. Poellot, E. Eloranta, Journal of Atmospheric and Oceanic Technology **25**(4), 547 (2008).
[6] B. T. Lottman, R. G. Frehlich, S. M. Hannon, S. W. Henderson, J. Atmos. Oceanic Technol. **18**(8), 1377 (2001).
[7] A. Ansmann, J. Fruntke, R. Engelmann, Atmos. Chem. Phys. **10**(16), 7845 (2010).
[8] J. Bühl, R. Leinweber, U. Görsdorf, M. Radenz, A. Ansmann, V. Lehmann, Atmos. Meas. Tech. **8**(8), 3527 (2015).
[9] Y. Peng, Y. Wu, C. Shen, H. Xu, J. Li, Remote Sensing **16**(12), 2212 (2024).
[10] F. Barbaresco, Ludovic Thobois, Agnès Dolfi-Bouteyre, Nicolas Jeannin, Richard Wilson, Matthieu Valla, Alexandre Hallermeyer, Patrick Feneyrou, Vincent Brion, Lucas Besson, Jean-Pierre Cariou, Luc Leviandier, Grégoire Pillet, Daniel Dolfi, URSI France JS 15, Journées Scientifiques 2015: Sonder la matière par les ondes électromagnétiques, Actes, URSI France, Mar 2015, Paris, France, 81 (2015).
[11] R. Pîrloagă, M. Adam, B. Antonescu, S. Andrei, S. Ştefan, Remote Sensing **15**(6), 1514 (2023).
[12] R. Pîrloagă, D. Ene, M. Boldeanu, B. Antonescu, E. J. O'Connor, S. Ştefan, Atmosphere **13**(9), 1445 (2022).
[13] M. Adam, Konstantinos Fragkos, Ioannis Binietoglou, Dongxiang Wang, Iwona S. Stachlewska, Livio Belegante, Victor Nicolae, Remote Sensing **14**(5), 1217 (2022).
[14] M. Adam, Konstantinos Fragkos, Stavros Solomos, Livio Belegante, Simona Andrei, Camelia Talianu, Luminița Mărmureanu, Bogdan Antonescu, Dragos Ene, Victor Nicolae, Vassilis Amiridis, Remote Sensing **14**(19), 4734 (2022).
[15] E. Carstea, K. Fragkos, Optoelectron. Adv. Mat. **18**(11-12), 562 (2024).
[16] L. Belegante, Camelia Talianu, Anca Nemuc, Victor Nicolae, G Ciocan, Flori Toanca, Ovidiu Gelu Tudose, Cristian Marian Radu, Doina Nicolae, J. Optoelectron. Adv. M. **26**(-10), 422 (2024).
[17] P. Kollias, B. A. Albrecht, R. Lhermitte, A. Savtchenko, J. Atmos. Sci. **58**(13), 1750 (2001).
[18] P. Kollias, B. A. Albrecht, F. D. Marks, J. Geophys. Res. **108**(D2), 2001JD002033 (2003).
[19] P. Kollias, J. Rémillard, E. Luke, W. Szyrmer, J. Geophys. Res. **116**(D13), D13201 (2011).
[20] M. Adam, A. Nemuc, R. Pîrloagă, F. Țoancă, E. O'Connor, J. Vasilescu, ACTRIS Cloud remote sensing data centre unit (CLU), Jun. 12, 2025.
[21] A. J. Illingworth, R. J. Hogan, E. J. O'connor, D. Bouniol, M. E. Brooks, J. Delanoë, D. P. Donovan, J. D. Eastment, N. Gaussiat, J. W. F. Goddard, M. Haeffelin, H. Klein Baltink, O. A. Krasnov, J. Pelon, J.-M. Piriou, A. Protat, H. W. J. Russchenberg, A. Seifert, A. M. Tompkins, G.-J. Van Zadelhoff, F. Vinit, U. Willén, D. R. Wilson, C. L. Wrench, Bulletin of the American Meteorological Society **88**(6), 883 (2007).
[22] R. B. Stull, Meteorology: for scientists and engineers, The University of British Columbia Vancouver, Canada, 2015.
[23] P. Kollias, S. Tanelli, A. Battaglia, A. Tatarevic, Journal of Atmospheric and Oceanic Technology **31**(2), 366 (2014).

*Corresponding author: anca@inoe.ro

ANNEX A – 11 December 2024

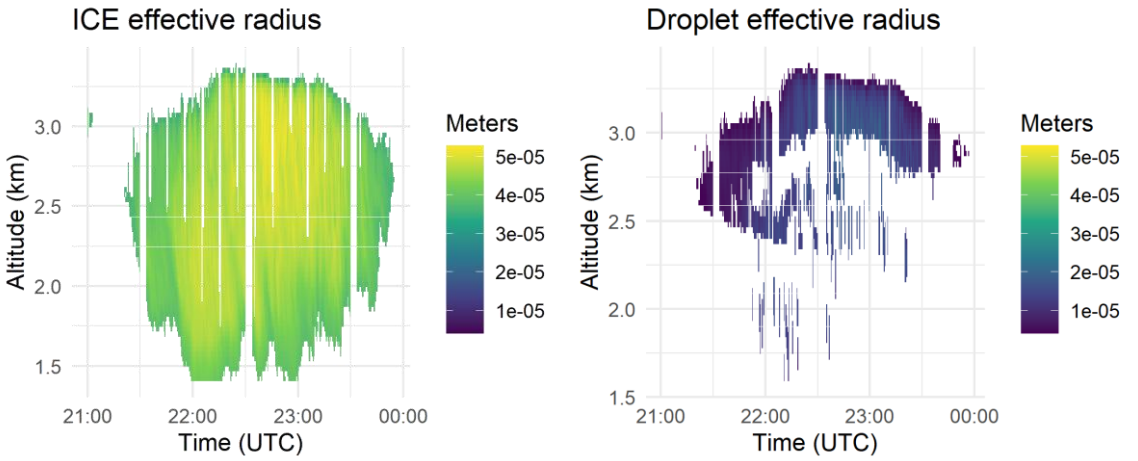

Fig. A1. (left) Ice effective radius and (right) droplet effective radius on 11 December 2024 (colour online)

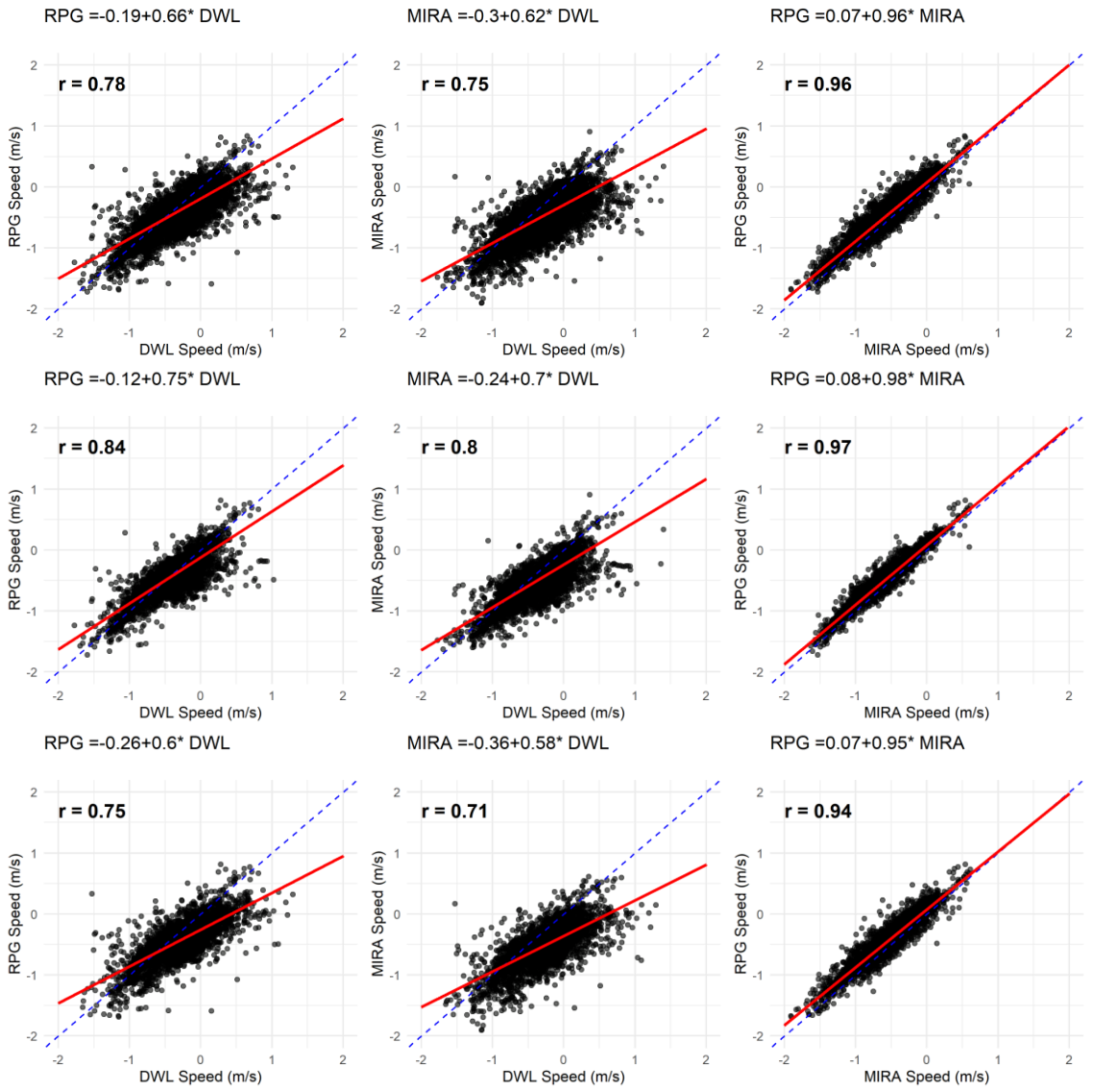

Fig. A2. Correlations between RPG and DWL (left), MIRA and DWL (middle), RPG and MIRA (right) when all data (top), ice particles data (middle) and mixed phase data (bottom) is considered. The data represent the 21:00—24:00 time interval on 11 December 2024 (colour online)

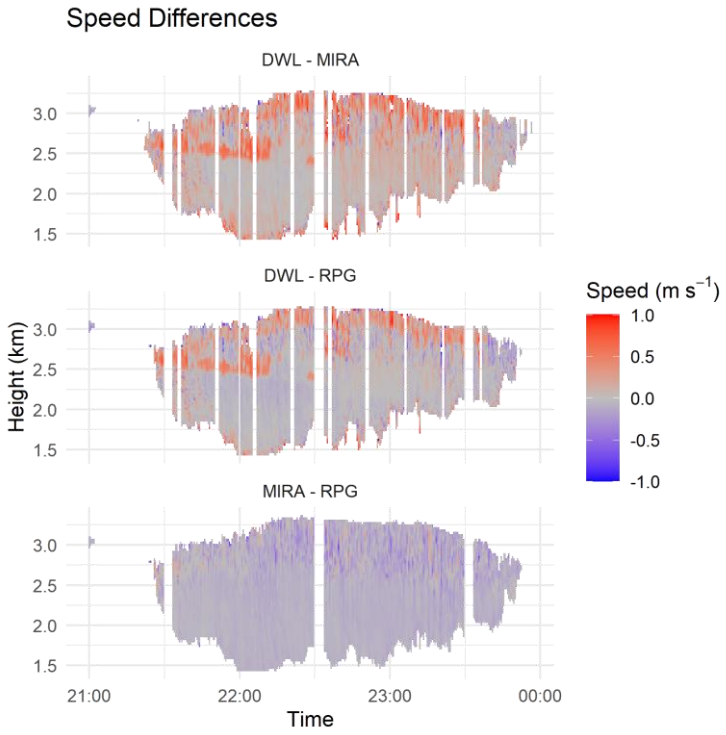

Fig. A3. Speed differences for all particles between DWL and MIRA radar (top), DWL and RPG radar (middle), MIRA and RPG radars (bottom) for low to mid-altitude cloud (1400—3500 meters altitude) in the 21:00—24:00 time interval on 11 December 2024 (colour online)

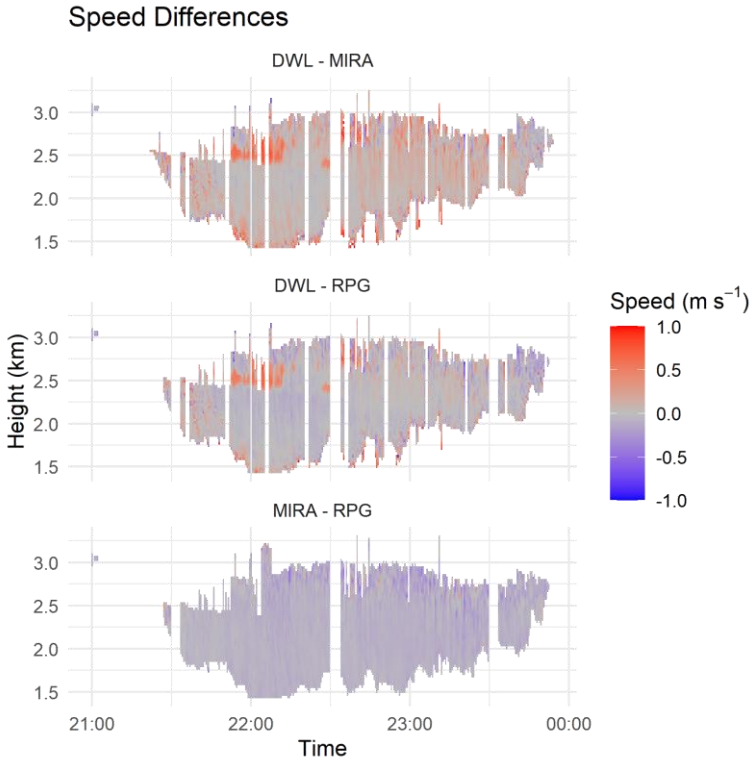

Fig. A4. Speed differences for ICE particles between DWL and MIRA radar (top), DWL and RPG radar (middle), MIRA and RPG radars (bottom) for low to mid-altitude cloud (1400—3500 meters altitude) in the 21:00—24:00 time interval on 11 December 2024 (colour online)

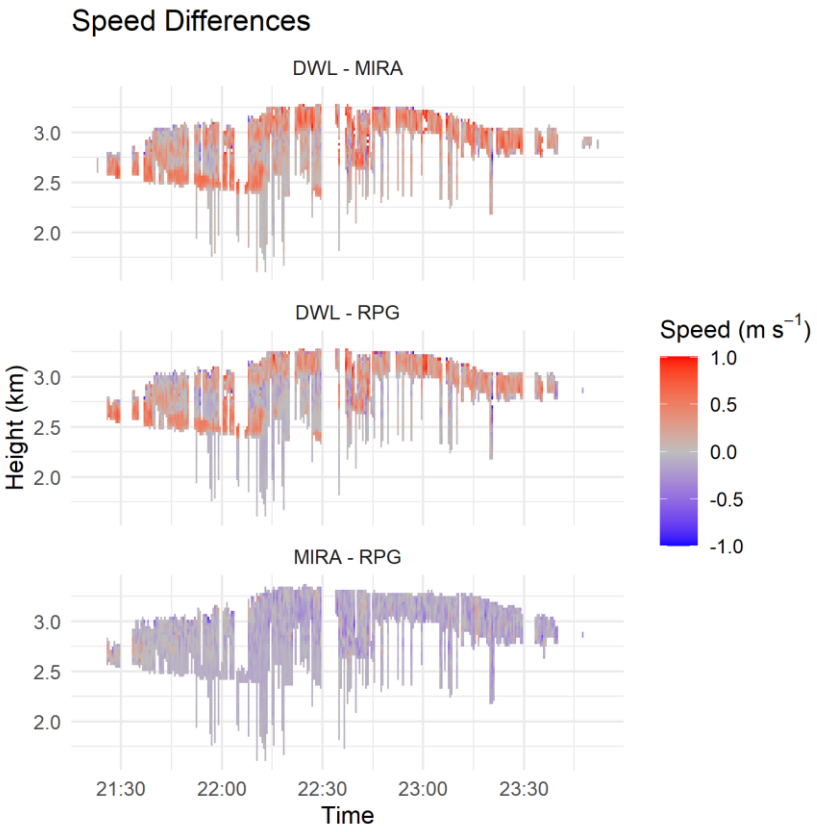

Fig. A5. Speed differences for mixed phased particles between DWL and MIRA radar (top), DWL and RPG radar (middle), MIRA and RPG radars (bottom) for low to mid-altitude cloud (1400—3500 meters altitude) in the 21:00—24:00 time interval on 11 December 2024 (colour online)

ANNEX B

I. 12 December 2024

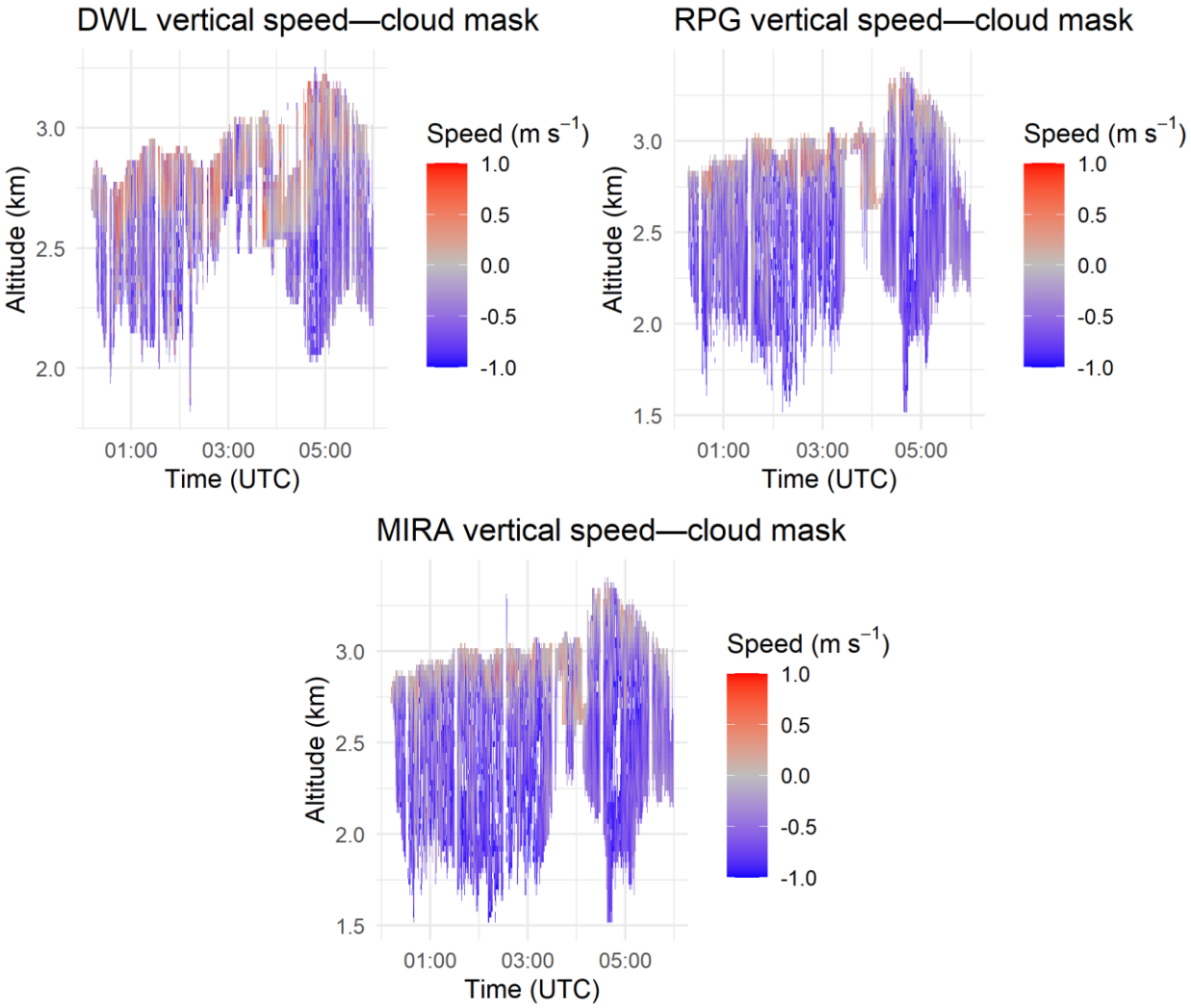

Fig. B1. Cloud masked vertical wind speeds measured by DWL (top), RPG cloud radar (middle) and MIRA cloud radar (bottom) for low to mid-altitude cloud (1500—3500 meters altitude) in the 00:00—06:00 time interval on 12 December 2024

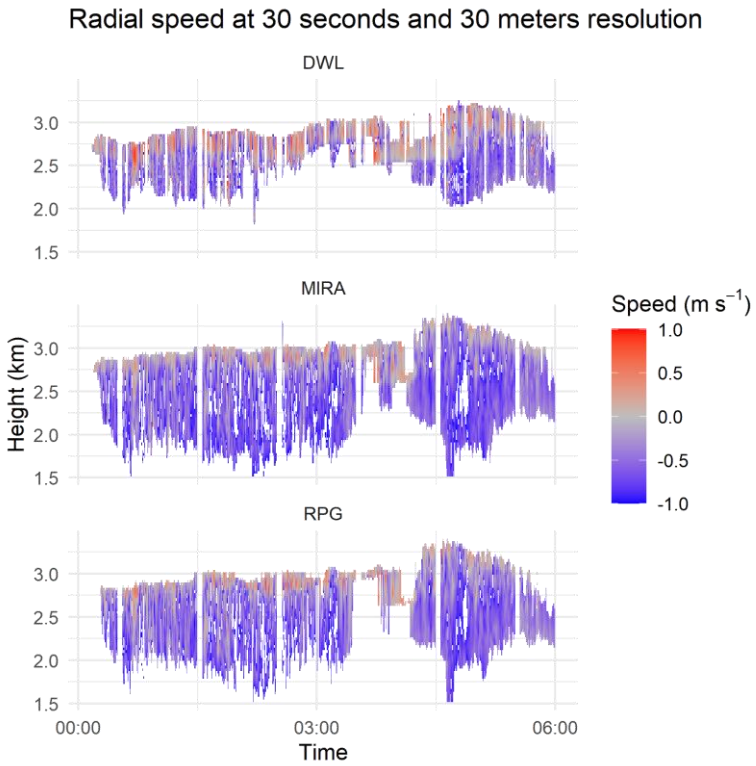

Fig. B2. Vertical speed profiles interpolated at the common resolution (30 seconds and 30 meters) for low to mid-altitude cloud (1500—3500 meters altitude) in the 00:00—06:00 time interval on 12 December 2024 (colour online)

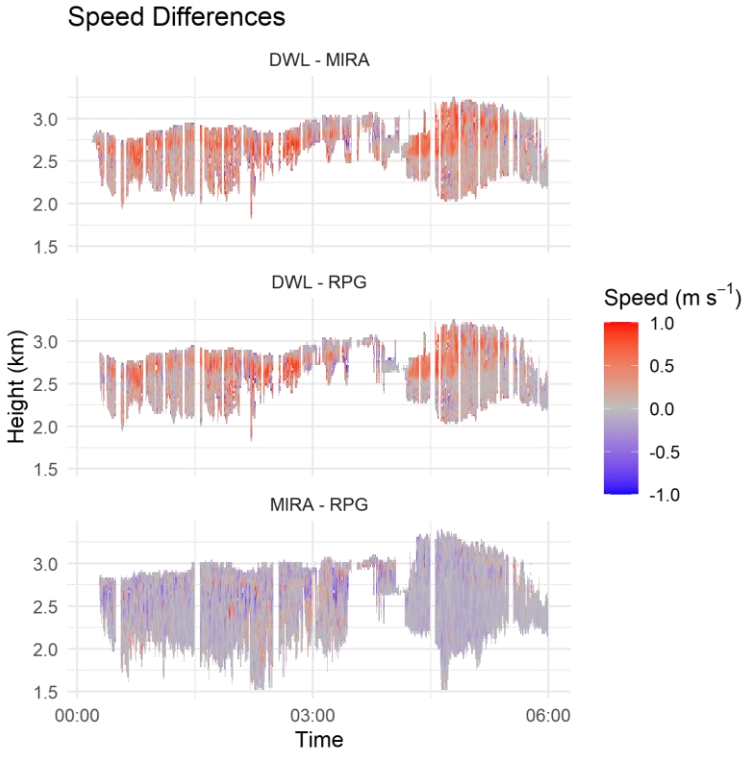

Fig. B3. Speed differences between DWL and MIRA radar (top), DWL and RPG radar (middle), MIRA and RPG radars (bottom) for low to mid-altitude cloud (1500—3500 meters altitude) in the 00:00—06:00 time interval on 12 December 2024 (colour online)

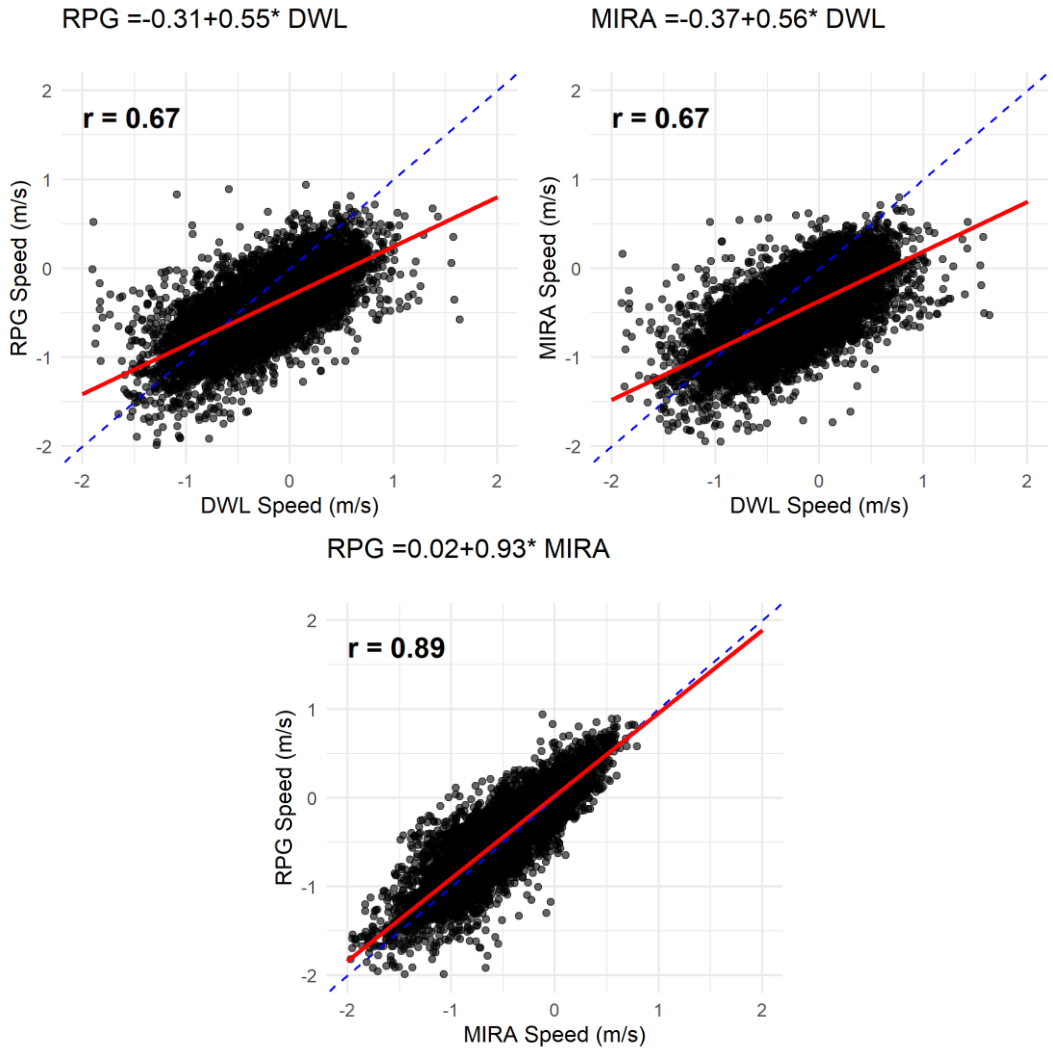

Fig. B4. Correlation graph between DWL and RPG radar (top), DWL and MIRA radar (middle), MIRA and RPG radars (bottom) for low to mid-altitude cloud (1500—3500 meters altitude) in the 00:00—06:00 time interval on 12 December 2024 (colour online)

II. 18 December 2024

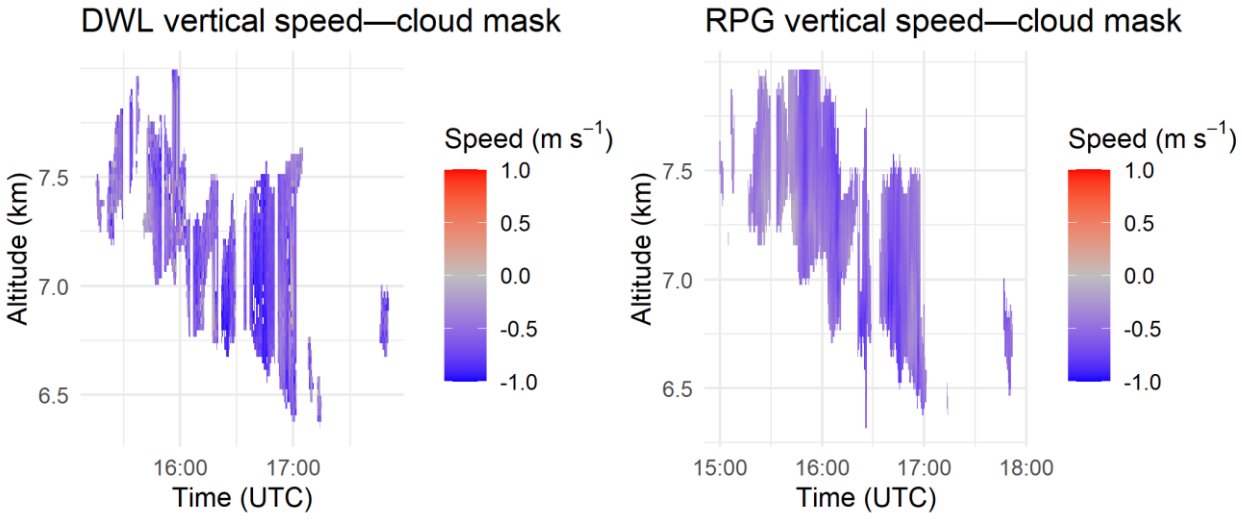

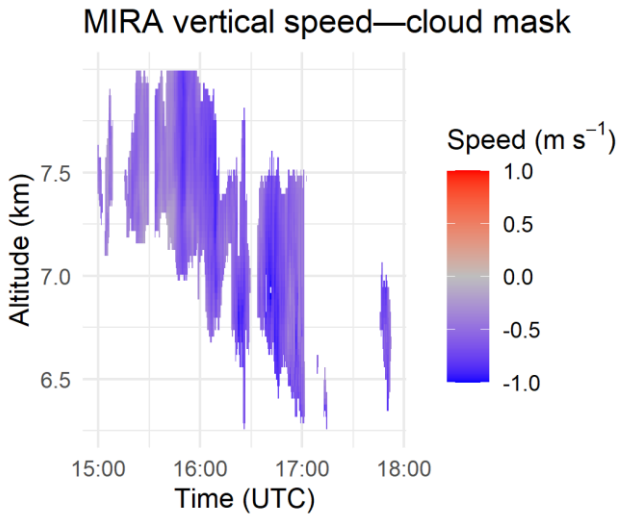

Fig. B5. Cloud masked vertical wind speeds measured by DWL (top), RPG cloud radar (middle) and MIRA cloud radar (bottom) for high cloud (6000—8000 meters altitude) in the 15:00—18:00 time interval on 18 December 2024 (colour online)

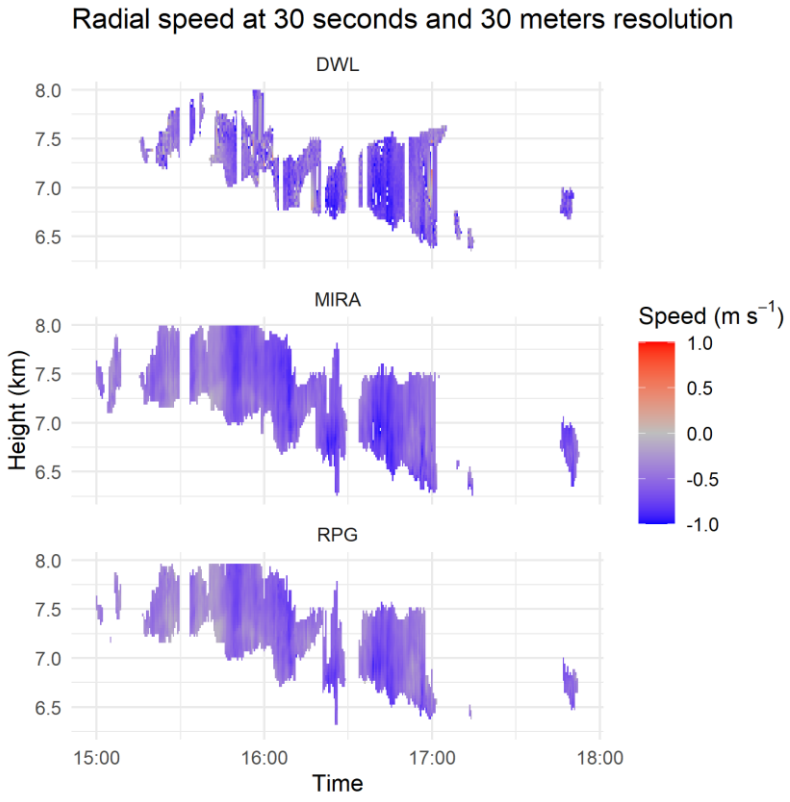

Fig. B6. Vertical speed profiles interpolated at the common resolution (30 seconds and 30 meters) for high cloud (6000—8000 meters altitude) in the 15:00—18:00 time interval on 18 December 2024 (colour online)

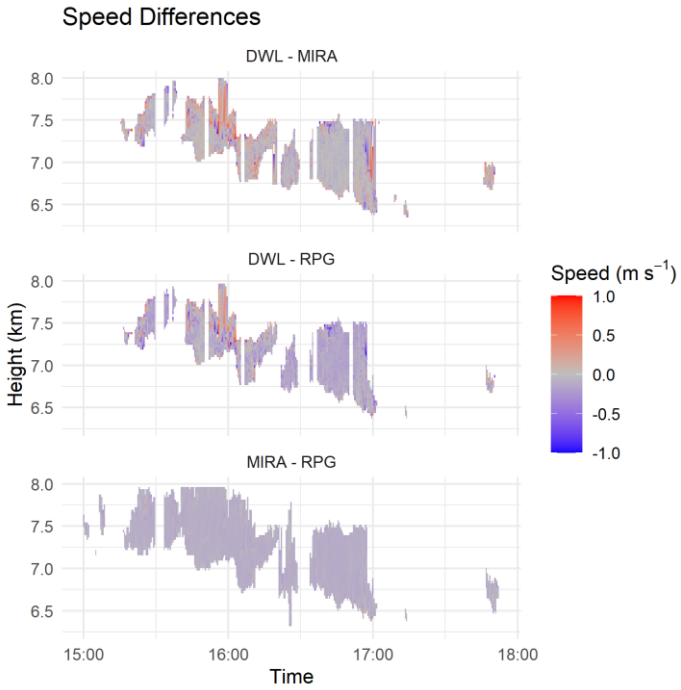

Fig. B7. Speed differences between DWL and MIRA radar (top), DWL and RPG radar (middle), MIRA and RPG radars (bottom) for high cloud (6000—8000 meters altitude) in the 15:00—18:00 time interval on 18 December 2024 (colour online)

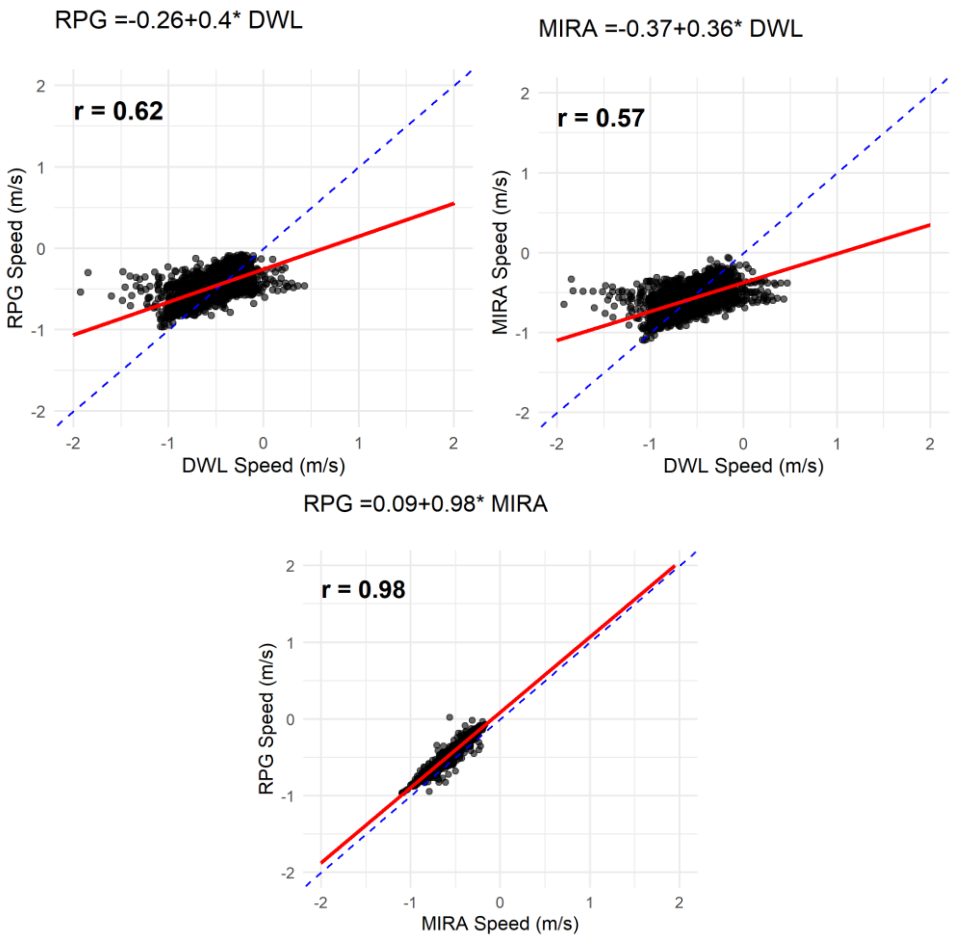

Fig. B8. Correlation graph between DWL and RPG radar (top), DWL and MIRA radar (middle), MIRA and RPG radars (bottom) for high cloud (6000—8000 meters altitude) in the 15:00—18:00 time interval on 18 December 2024 (colour online)

III. 14 February 2025

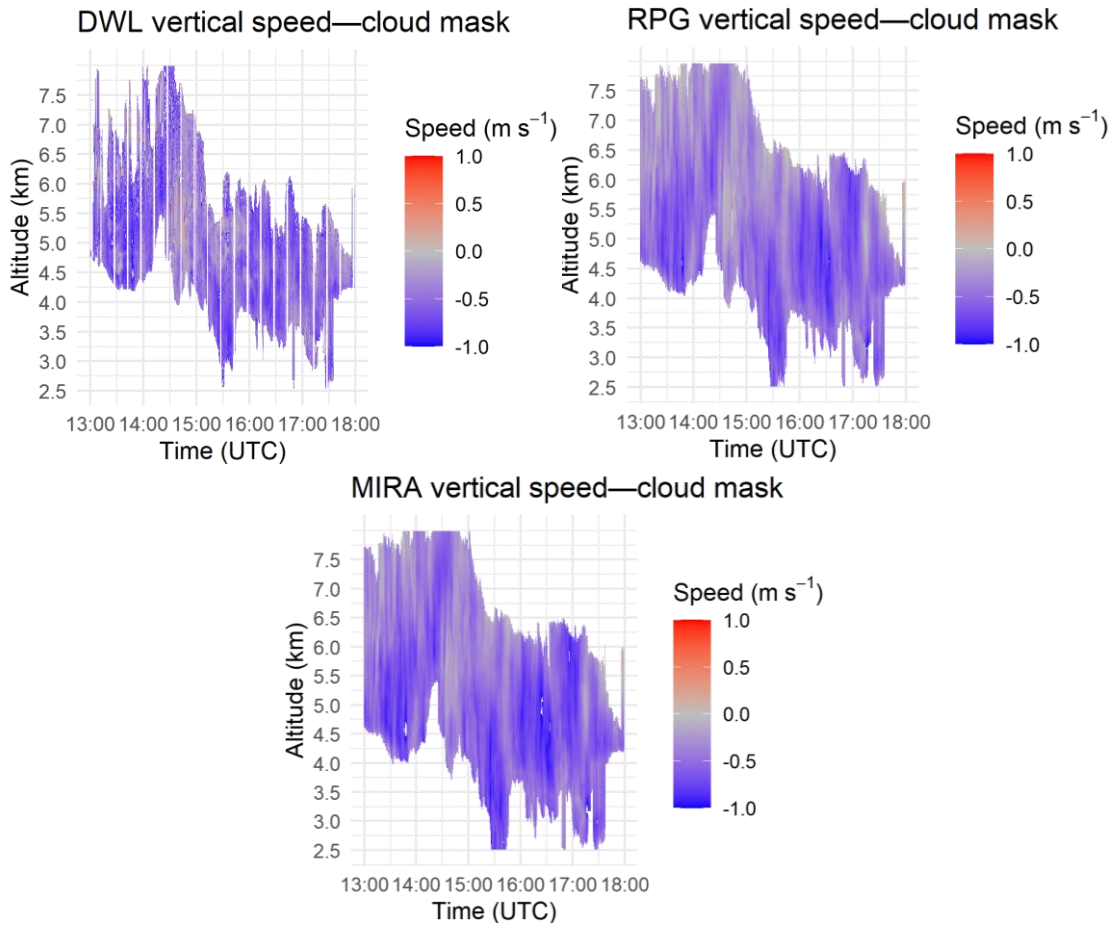

Fig. B9. Cloud masked vertical wind speeds measured by DWL (top), RPG cloud radar (middle) and MIRA cloud radar (bottom) for extended towering cloud (2500—8000 meters altitude) in the 13:00—18:00 time interval on 14 February 2025 (colour online)

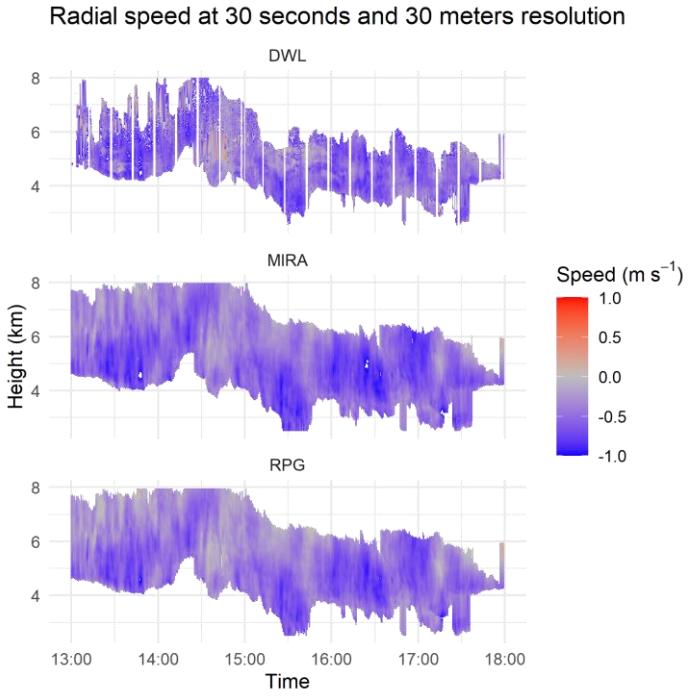

Fig. B10. Vertical speed profiles interpolated at the common resolution (30 seconds and 30 meters) for extended towering cloud (2500—8000 meters altitude) in the 13:00—18:00 time interval on 14 February 2025 (colour online)

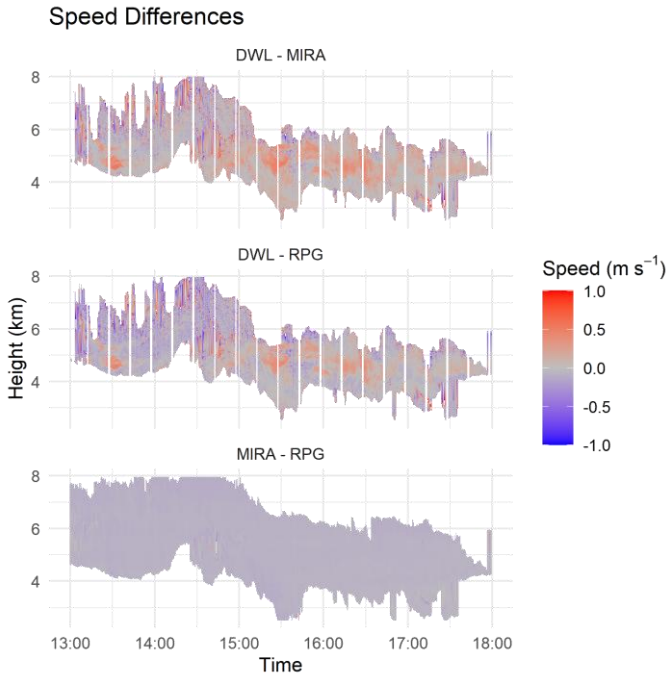

Fig. B11. Speed differences between DWL and MIRA radar (top), DWL and RPG radar (middle), MIRA and RPG radars (bottom) for extended towering cloud (2500—8000 meters altitude) in the 13:00—18:00 time interval on 14 February 2025 (colour online)

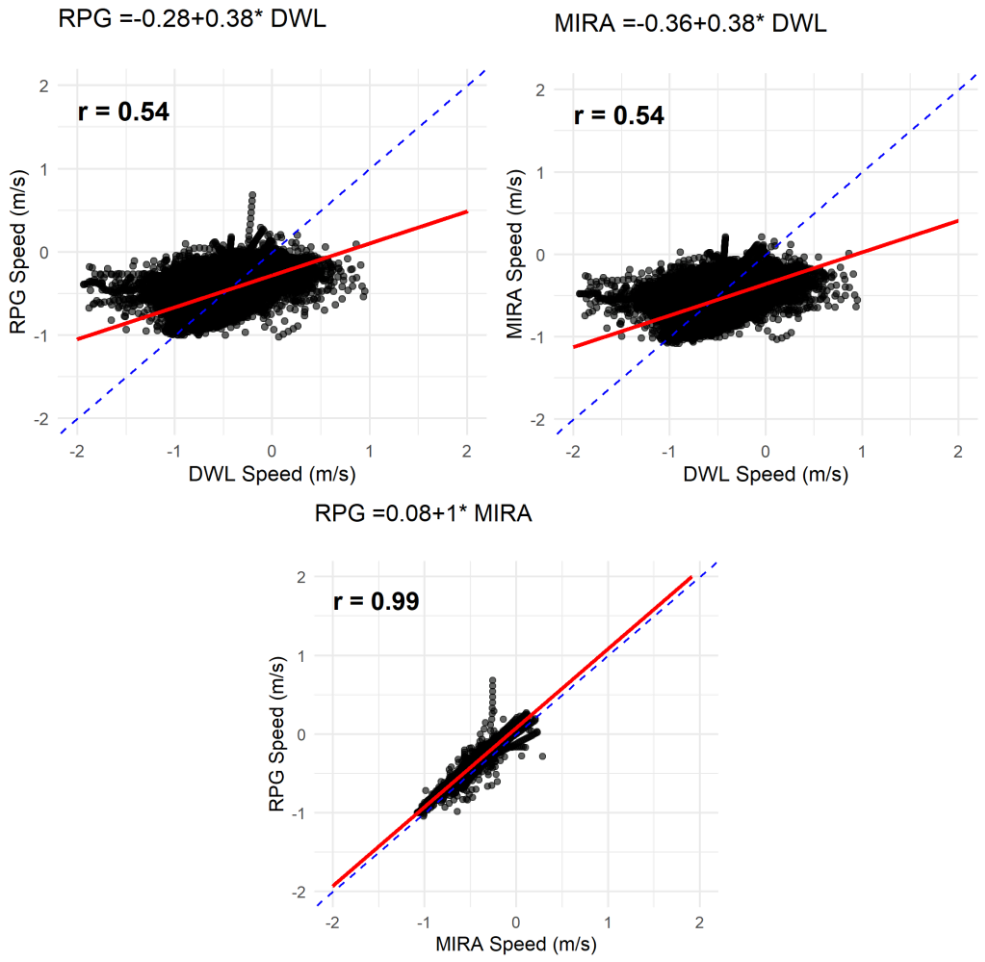

Fig. B12. Correlation graph between DWL and RPG radar (top), DWL and MIRA radar (middle), MIRA and RPG radars (bottom) for extended towering cloud (2500—8000 meters altitude) in the 13:00—18:00 time interval on 14 February 2025 (colour online)